

*Citation for published version:*

Díaz de León–Ortega, R, D'Arcy, DM, Lamprou, DA & Fotaki, N 2021, 'In vitro - in vivo relations for the parenteral liposomal formulation of Amphotericin B: A clinically relevant approach with PBPK modeling', *European Journal of Pharmaceutics and Biopharmaceutics*, vol. 159, pp. 177-187.  
<https://doi.org/10.1016/j.ejpb.2020.03.001>

*DOI:*

[10.1016/j.ejpb.2020.03.001](https://doi.org/10.1016/j.ejpb.2020.03.001)

*Publication date:*

2021

*Document Version*

Peer reviewed version

[Link to publication](#)

*Publisher Rights*

CC BY-NC-ND

**University of Bath**

**Alternative formats**

If you require this document in an alternative format, please contact:  
[openaccess@bath.ac.uk](mailto:openaccess@bath.ac.uk)

**General rights**

Copyright and moral rights for the publications made accessible in the public portal are retained by the authors and/or other copyright owners and it is a condition of accessing publications that users recognise and abide by the legal requirements associated with these rights.

**Take down policy**

If you believe that this document breaches copyright please contact us providing details, and we will remove access to the work immediately and investigate your claim.

*In vitro in vivo* relations for the parenteral liposomal formulation of Amphotericin B. Part 2: A clinically relevant approach with PBPK modeling

R. Díaz de León–Ortega<sup>1</sup>, D. M. D'Arcy<sup>2</sup>, D.A. Lamprou<sup>3</sup>, N. Fotaki<sup>1,\*</sup>

<sup>1</sup> Department of Pharmacy and Pharmacology, University of Bath, Bath, United Kingdom

<sup>2</sup> School of Pharmacy and Pharmaceutical Sciences, Trinity College Dublin, Dublin 2, Ireland

<sup>3</sup> School of Pharmacy, Queen's University Belfast, Belfast, United Kingdom

\* Corresponding Author

Dr Nikoletta Fotaki

Department of Pharmacy and Pharmacology

University of Bath

Claverton Down

Bath, BA2 7AY

United Kingdom

Tel. +44 1225 386728

Fax: +44 1225 386114

E-mail: [n.fotaki@bath.ac.uk](mailto:n.fotaki@bath.ac.uk)

## Abstract

*In vitro* release testing is a useful tool for the quality control of controlled release parenteral formulations, but *in vitro* release test conditions that reflect or are able to predict the *in vivo* performance are advantageous. Therefore, it is important to investigate the factors that could affect drug release from formulations and relate them to *in vivo* performance. In this study the effect of media composition including albumin presence, type of buffer and hydrodynamics on drug release were evaluated on a liposomal Amphotericin B formulation (Ambisome®). A physiologically based pharmacokinetic (PBPK) model was developed using plasma concentration profiles from healthy subjects, in order to investigate the impact of each variable from the *in vitro* release tests on the prediction of the *in vivo* performance. It was found that albumin presence was the most important factor for the release of Amphotericin B from Ambisome®; both hydrodynamics setups, coupled with the PBPK model, had comparable predictive ability for simulating *in vivo* plasma concentration profiles. The PBPK model was extrapolated to a hypothetical hypoalbuminaemic population and the Amphotericin B plasma concentration and its activity against fungal cells were simulated. Selected *in vitro* release tests for these controlled release parenteral formulations were able to predict the *in vivo* AmB exposure, and this PBPK driven approach to release test development could benefit development of such formulations.

## Keywords:

Amphotericin B; liposomes; PBPK; modeling; *in vitro*; release; PBPKPD; clinically; relevant

## 1. Introduction

A recent consensus document arising from a workshop dedicated to bringing consistency to terminology used in dissolution testing has defined a clinically relevant *in vitro* release test as the implication of a link between the *in vitro* release and the *in vivo* performance [1]. In order to establish a clinically relevant test, it is important to understand how the test conditions (e.g. media composition and hydrodynamics) affect the *in vitro* release from the formulation. In some cases, the information obtained from *the in vitro* release tests is not enough to explain the *in vivo* behaviour of the formulation and the released drug, and a mechanistic understanding of the *in vivo* performance is required [2]. This can be achieved by the use of physiologically based pharmacokinetic (PBPK) modeling. The general concept of PBPK modeling is to mathematically describe relevant physiological, physicochemical, and biochemical processes that determine the pharmacokinetic behaviour of a compound [3-5]. PBPK modeling and simulation are currently a trending tendency and commercial software are available (for example, Gastro-Plus®, simCYP® or PK-Sim® [6]). PBPK modeling is now accepted by regulatory agencies [7]. The Food and Drug Administration (FDA) have published the “Physiologically Based Pharmacokinetic Analyses — Format and Content (Guidance for Industry) [8]” and the European Medicines Agency (EMA) the “Guideline on the qualification and reporting of physiologically based pharmacokinetic (PBPK) modelling and simulation [9]”. A PBPK model can be developed considering 4 stages: i) setting the model equations to represent the system, ii) input data to the model, iii) perform the simulation and iv) model validation (observed vs simulated data, parameter sensitivity analysis) [2]. A sensitivity analysis allows the identification of the parameters that have the greatest influence on the simulation [10, 11].

A biopredictive release method consists of *in vitro* release testing conditions that, coupled with mathematical modeling, are capable of predicting *in vivo* pharmacokinetic profiles [1]. PBPK

modeling can be extrapolated to simulate diseased populations, and could thus be used for example for hypoalbuminaemic patients (plasma albumin < 25 g/L [12]), in order to investigate the pharmacodynamics (PD) of the drug [13]. Hypoalbuminaemia can be observed in critically ill patients with sepsis, who may be among the patient cohort administered AmB.

PBPK/PD models integrate the movement of the drug in the body with its pharmacological activity [13]. In antimicrobial therapy, the pharmacological effect is the activity against an infectious agent [14-16]. If a PBPK/PD model is used to evaluate the antimicrobial activity, for many antimicrobial agents the microbial killing is considered to be dependent on the PK profile of antimicrobial concentration in plasma [10, 17]. Amphotericin B (AmB) is a poorly soluble highly protein bound drug used in the treatment of severe systemic fungal disease (e.g. *Candida sp.*, *Aspergillus sp.* [18, 19]) and is commercially available as parenteral lipid formulations (including the liposomal formulation Ambisome®) for intravenous administration. The development of PBPK models for Amphotericin B in mice and rats after the administration of Fungizone® (colloidal AmB) and Ambisome® have been reported [20, 21], which showed good predictive performance after being extrapolated to humans. For PBPK modeling of Ambisome®, the uptake of particles by macrophage cells in organs like the liver and spleen, were taken into account by using a saturable model. When this model was developed, the authors reported that there was no *in vitro* AmB release data available and they determined a value from fitting the model to the data with a release rate constant of 0.0035 h<sup>-1</sup> (in all the tissues) with an initial rapid release of the 8% of the dose in humans [20, 21].

The aims of this study were i) to investigate how the presence of albumin in clinically relevant media containing physiological surfactants (bile salts – phospholipids) [22]) combined with a biorelevant hydrodynamic environment [23], impacts on the release of AmB from Ambisome®; ii) to develop a PBPK model to predict plasma drug concentrations in healthy subjects; iii) coupled with the use of the PBPK model, to guide the development of a biopredictive *in vitro*

release test for the liposomal AmB formulation Ambisome<sup>®</sup>; iv) to extrapolate the PBPK model to a hypoalbuminaemic population to build a PBPK/PD model to simulate the pharmacological effect of AmB on fungal cells present in hypoalbuminaemic plasma vs plasma with normal albumin levels.

## **2. Materials and Methods**

### **2.1. Materials**

AmB analytical standard (87.8%), methanol (MeOH) high performance liquid chromatography (HPLC) grade, formic acid mass spectrometry grade, Sabouraud dextrose (SBD) broth, NaOH, MgCl<sub>2</sub>, CaCl<sub>2</sub>, and NaHCO<sub>3</sub> were obtained from Sigma Aldrich (Germany); AmB API powder (85%) from Cayman Chemical (USA); bovine serum albumin protease free powder fraction V (BSA), dimethyl sulfoxide (DMSO), dextrose, sodium dodecyl sulphate (SLS), Na<sub>2</sub>HPO<sub>4</sub>, NaH<sub>2</sub>PO<sub>4</sub>, KH<sub>2</sub>PO<sub>4</sub>, NaCl and KCl from Fisher Scientific (USA); phosphatidylcholine (PL) from egg from Lipoid GmbH (Ludwigshafen, Germany); sodium taurocholate (BS) from Prodotti Chimici e Alimentaria (Italy); Sabouraud dextrose (SBD) agar was obtained from Oxoid (UK), 25 mL sterile universal culture tubes were obtained from Sterilin Thermo Scientific (UK); 10 µL plastic loops from Microspec (UK); GF/D (pore size 2.7 µm, 25 mm diameter) and GF/F (pore size 0.7 µm, 25 mm diameter) filters from Whatman (UK); regenerated cellulose (RC) filters 0.45 µm 13 mm diameter from Cronus (UK); cellulose ester dialysis tubing of 300 kDa MWCO from Spectrum Labs (USA), C18 Sep – Pak<sup>®</sup> Vac 3cc (500 mg) solid phase extraction (SPE) column from Waters (USA) and Ambisome<sup>®</sup> liposomal AmB formulation from Gilead (Gilead, UK).

### **2.2. Sample treatment of AmB in release media**

The sample treatment of AmB was described previously [23]. Briefly, the SPE method to separate "liposomal AmB" (AmB still entrapped in the liposome) from "released AmB" (AmB

released from the liposome) was modified from Egger et al [24]. The SPE column was conditioned with methanol, followed by water. 1.0 mL of sample was passed through the column and the eluate was collected in a clean vial (liposomal AmB), the column was washed with 2.0 mL of water and collected in the same tube. 1.0 mL of methanol was flushed through the column to elute the AmB retained in the column (released AmB). In the case of samples with proteins, proteins were precipitated by adding 2 volumes of methanol to 1 volume of the sample followed by mixing in a vortex mixer, then centrifuged for 10 minutes at 12000 rpm and 5°C. The supernatant was filtered through a 0.45 µm RC filter before injection to the HPLC.

### **2.3. Chromatographic conditions for the analysis of AmB from release media**

The chromatographic method to quantify AmB was described previously [25]. Briefly, AmB was quantified by HPLC analysis using a Hewlett Packard Series 1100 equipped with an auto sampler, temperature regulated column compartment, quaternary pump and diode array detector (DAD detector) (Agilent Technologies). The column was a C18 Waters Sunfire Column (Ireland) 150 x 46 mm 5 µm. The temperature of the column compartment was set at 25°C. The mobile phase consisted of formate buffer 50 mM pH = 3.2: MeOH (27.5:72.5, v/v); the flow rate was 1 mL/min and analysis was performed with the DAD detector at  $\lambda = 406$  nm. The UV spectrum was recorded from 300 to 450 nm. Quantification of AmB in samples was made based on calibration curves. Freshly prepared standard solutions (0.5 – 15 µg/mL) in the corresponding medium were prepared by appropriate dilution of a 500 µg/mL stock solution of AmB analytical standard in 1:1 MeOH: DMSO v/v. The limit of detection and the limit of quantification were 0.12 and 0.37 µg/mL, respectively.

### **2.4. *In vitro* release studies of AmB from Ambisome®**

The factors investigated for the development of the *in vitro* release studies were: i. the composition of the clinically relevant media with biorelevant surfactants (media AmB solubility value equivalent to that observed in plasma from healthy subjects [22]); media composition factors explored were: type of buffer and BSA concentration, and ii. the hydrodynamic conditions in terms of the apparatus used i.e. sample and separate (bottle/stirrer) or continuous flow (flow through cell apparatus).

Media compositions were PBS BS 19.8 mM PL 7.9 mM and KRB BS 20.0 mM PL 4.0 mM, with and without BSA 4.0% w/v. Media preparation was as previously described [22]. Briefly, BS were weighed and dissolved in buffer and then PL from a stock solution of 100 mg/mL in dichloromethane was added. Organic solvents were evaporated with a rotary evaporator set at 40°C and attached to a vacuum pump. The pressure was decreased from 650 mbar by steps of 70 mbar every two minutes to 100 mbar, where the pressure was maintained for 10 minutes. When included in the medium, BSA was added after the evaporation of the organic solvents.

#### **2.4.1. Sample and separate method (bottle/stirrer setup)**

The sample and separate method was described previously [23]. Briefly, Ambisome® powder (0.5 mg AmB) was placed into a 100 mL glass bottle with 30 mL of release medium and stirred with a magnetic stirrer at 37°C. Release studies were performed based on a two-level factorial design of experiments (DoE). The factors investigated (composition of release media and agitation conditions) are shown in Table 1; the combination of all the factors resulted in eight experimental setups.

The agitation rates in the bottle/stirrer setup were selected based on the linear velocity of the stirrer edge, which at 130 rpm (10.2 cm/s) is comparable to the linear flow velocities in vein/artries and at 380 rpm (29.5 cm/s) to flow velocities in the aorta [23]. Sampling times were 1, 2, 4, 6, 8, and 12 h and after sample treatment (SPE and protein precipitation), samples



were injected to the HPLC and AmB concentration in the samples was determined. All experiments were performed in triplicate.

#### **2.4.2. Continuous flow (flow through cell apparatus)**

The flow-through apparatus setup was described previously [23]. Briefly, AmB release studies were carried out in a flow-through dissolution apparatus (Sotax CE7 smart connected to a Sotax piston pump CP7, Sotax, Aesch Switzerland) operated in the closed mode [26]. A 5 mm ruby glass bead was positioned at the bottom of the cell (large cell: 22.6 mm diameter). The dialysis membrane was placed into the flow through cell apparatus dialysis adapter and Ambisome<sup>®</sup> powder (0.5 mg AmB) was placed into the membrane with 1 mL of the release medium. Glass fibre filters (GF/D, GF/F) were positioned at the top of the cell. The release studies were based on a two level factorial DoE, where the velocities used were considered biorelevant: “Low velocity” (flow rate: 8 mL/min) has an average linear velocity comparable to capillary flow and “High velocity” (flow rate: 35 mL/min) is comparable to intermediate capillary-vein flow [23] and BSA presence (4.0% w/v) or not were the factors investigated. 36 mL of KRB BS 20.0 mM PL 4.0 mM (with or without BSA) were used in order to simulate the equivalent volume available on administration of 1 mg/kg of AmB as Amphotericin B<sup>®</sup> to a 70 kg subject (assuming 5 L of blood volume). Furthermore, as the 36 mL volume used does not allow for distribution as would happen *in vivo*, it represents an extreme case in terms of available volume.

#### **2.5. Release data treatment**

The release data treatment was described previously [23]. Briefly, for the studies with the sample and separate method, % AmB released over time was calculated based on the % AmB still entrapped in the liposomes at the time of sampling ( $\%AmB_{liposomal}$ ) (Eq 1) to construct

the calculated  $\%AmB_{released}$  profile.  $\%AmB_{released} = \%AmB_{initial} - \%AmB_{liposomal}$

(Eq 1)

where  $\%AmB_{initial}$  is the mass of AmB placed into the reservoir initially (100%) and

$\%AmB_{released}$  is the calculated AmB percent released.

For the studies with the continuous flow setup the  $\%AmB_{released(obs)}$  over time was corrected

for degradation using Eq 2 to construct the calculated  $\%AmB_{released}$  profile.

$$\%AmB_{released} = \%AmB_{released(obs)} + k_{deg} * AUC_{0-t} \quad (\text{Eq 2})$$

where  $\%AmB_{released}$  is the corrected % AmB released accounting for degradation,

$\%AmB_{released(obs)}$  is the % AmB released at time  $t$ ,  $AUC_{0-t}$  is the Area Under the Curve of

the observed concentration – time curve from time 0 to time  $t$  and  $k_{deg}$  is the degradation rate

constant obtained from the degradation experiments [22].

The AmB release rate constant ( $k_{rel}$ ) from Ambisome<sup>®</sup> was obtained from first order fitting

of calculated  $\%AmB_{released}$  individual profiles (Equation 3) and mean and standard deviation

values were calculated (GraphPad Prism 7, GraphPad Software, Inc, USA).

$$\%AmB_{released} = \%AmB_{releasedmax} * (1 - e^{-k_{rel}t}) \quad (\text{Equation 3}),$$

where  $\%AmB_{releasedmax}$  is the maximum AmB percent released and  $t$  is time.

## 2.6. Atomic Force Microscopy (AFM) studies

To further investigate the effect of the clinically relevant media components (e.g. BS, PL and

BSA) on the liposomes, AFM studies were performed. The AFM methodology has been

described previously [23]. Ambisome<sup>®</sup> liposomes were incubated in KRB BS 20.0 mM PL 4.0

mM BSA 4.0% w/v (for 30 min) and in KRB BS 20.0mM PL 4.0 mM (for 5 min; a shorter

period of incubation was set in order to reflect the fast release of AmB from the liposomes

observed in the absence of BSA). After the incubation time, samples were centrifuged for 30 min at 13,300 rpm in an Eppendorf centrifuge, the supernatant was discarded and the pellet was dried under vacuum. The pellets were diluted with 1 mL of HPLC water, and then 10  $\mu$ L of the liposomal solution was placed on a freshly cleaved mica surface (1.5 cm  $\times$  1.5 cm; G250-2 Mica sheets 1"  $\times$  1"  $\times$  0.006"; Agar Scientific Ltd., Essex, UK). The sample was then air-dried for  $\sim$ 30 min and imaged immediately by scanning the mica surface in air under ambient conditions using a Bruker MultiMode 8 Scanning Probe Microscope (Bruker, Billerica, Massachusetts, USA) operated on Peak Force QNM mode. The AFM measurements were obtained using ScanAsyst-air probes (Bruker, Billerica, Massachusetts, US); the spring constant was calibrated by thermal tune (Nominal 0.4 N m<sup>-1</sup>) and the deflection sensitivity calibrated using a silica wafer. AFM scans were acquired at a resolution of 512  $\times$  512 pixels at scan rate of 1 Hz, and produced topographic images of the samples in which the brightness of features increases as a function of height. The raw image data were processed using Bruker Nanoscope Analysis (version 1.5), and height images were flattened to remove sample tilt and scanner bow. The surface roughness ( $R_a$ ) of each substrate was determined by using Nanoscope Analysis' algorithm to analyse several scans of the surface from different locations ( $n = 20$ ). AFM images were collected from random spot surface sampling (at least four areas).

## **2.7. PBPK modeling for Ambisome® administration to healthy subjects**

### **2.7.1 Data for PBPK modeling.**

Published data of plasma concentration profiles from a population of 5 healthy subjects (4 males, 1 female; ages from 33 to 65 years; height from 1.61 to 1.68 m; and weight from 68 to 86 kg) administered 2.0 mg/kg of Ambisome® by intravenous infusion over 2 h where the "liposomal AmB" and "released AmB" were quantified [27, 28], were digitalized with Webplot

digitalizer 3.8 software. "Liposomal AmB" and "released AmB" distribution, clearance, protein binding and physicochemical properties are shown in Table 2.

The PK parameters (distribution, clearance and protein binding) for "released AmB" were as reported by Kagan et al. after administration of the colloidal AmB formulation Fungizone® [21] (Table 2). Protein binding was characterized by  $k_{diss}$  (equilibrium dissociation constant). The nominal glomerular filtration rate (GFR) for AmB was 0.08 mL/min/kg as calculated using Eq 4, based on a fraction unbound of 0.05. This value was used to calculate the GFR fraction for the "liposomal AmB" and "released AmB".

$$Nomimal\ GFR = fraction\ unbound\ (albumin) * (120\ mL/min) * (1/73\ kg) \quad Eq\ 4.$$

The biliary elimination rate constant was calculated using Eq 5.

$$k_{bil} = (Cl_{biliary}/distributuion\ volume)(60\ min/1\ h) \quad Eq\ 5.$$

For the development of the model, "liposomal AmB" was assumed to behave as a molecule as the concentration of AmB is what is quantified in the *in vivo* studies and not the concentration or amount of liposomes.

An "immune" enzyme was added for the "liposomal AmB" to account for the removal of circulation of the "liposomal AmB" by the macrophages of the immune system. The enzyme was set to be located in the plasma, liver and spleen. The fraction unbound value for the "liposomal AmB" was hypothesized to be smaller than 0.95 based on the reported interaction between albumin and liposomes [38-40]. All the other parameters were left as software default values.

## **2.7.2. Workflow for PBPK modeling of Ambisome®**

The workflow for the PBPK modeling to describe the pharmacokinetics of "liposomal AmB" and "released AmB" in a healthy individual after the administration of the Ambisome® is presented in Figure 1.

PBPK modeling was performed with PKSim® 7.2.1 (Bayer, Germany) and MoBi® 7.2 (Bayer, Germany). The five parameters listed in Figure 1 were optimized simultaneously with the MoBi® built in function "Parameter identification" using an algorithm based on Monte Carlo methods and the default software setup (the Parameter identification tool varies selected input parameters in a given range to identify the best values to obtain output simulated curves similar to the observed curves). The *in vivo* release of AmB from the liposomes was set to occur only in plasma ( $k_{rel-iv}$ ).

Comparing the developed PBPK model in this study with that reported by Kagan et al [21], there were some differences: i) this model was developed in order to link the *in vitro* release data to the observed plasma concentration data while Kagan and co-workers developed their model to have a better understanding of AmB PK in order to improve dosing; ii) the model developed by Kagan et al. assumed that release of AmB took place in all compartments [21] while in this study, the release was modelled in plasma only.

Sensitivity analysis was performed on all the parameters of the model (PK parameter estimates and physicochemical properties of "liposomal AmB" and "released AmB") except for the molecular weight and the pKa values of "released AmB". The parameters and the range in which the sensitivity analysis was evaluated are presented in Table 3.

The ranges were selected as follows: logP of "liposomal AmB" and "released AmB":  $\pm 1$  log unit of the optimized value, immune enzyme of "liposomal AmB":  $\pm 1 \text{ h}^{-1}$  of the optimized value, aqueous solubility of "released AmB": the range was selected to cover the solubility values reported in the literature [33-35], aqueous solubility of "liposomal AmB":  $\pm 200 \text{ }\mu\text{g/mL}$

in order to cover a wide range as the solubility value was calculated by considering the total amount of formulation powder in a vial (14.5 g), dissolved in 50 mL of water (Table 2); for radius solute ("liposomal AmB"), biliary clearance ("liposomal AmB" and "released AmB"),  $k_{diss}$  of lipoprotein B (APOB) and alpha1-acid glycoprotein (AAG1) the interval was  $\pm 50\%$  of the literature value (Table 2 and 3). The GFR fraction ("liposomal AmB" and "released AmB") was investigated ranging from 0 to 1; and the unbound to protein fraction ("liposomal AmB" and "released AmB") from 0.05 to 0.95.  $k_{rel-iv}$  was investigated in the interval of the  $k_{rel}$  found in the *in vitro* tests (Table 3).  $AUC_{0-24h}$  of both liposomal and released AmB was used as response to evaluate the effect of the parameters investigated. Sensitivity analysis was performed with the MoBi Toolbox for R esqLABS version 7.2.1 (esq LABS, Germany). All the intervals tested, were normalized to 0 – 1 for clarity of presentation.

After the sensitivity analysis, the model was applied to the population described in section 2.7.1. The variability (standard deviation) for the parameters input into the model was as described in Table 2. As the values of  $k_{rel-iv}$  and specific clearance for the immune removal "enzyme" were obtained by parameter identification and there are no reported values for their variability, 20% of the identified value was used as standard deviation.

### **2.7.3. Evaluation of the *in vitro* tests using PBPK modeling**

The *in vitro*  $k_{rel}$  (Mean  $\pm$  SD) obtained from the *in vitro* release profiles of AmB from Ambisome<sup>®</sup> were input to the validated PBPK model in order to predict the observed *in vivo* AmB ("liposomal AmB" and "released AmB") plasma concentration profiles. The  $AUC_{0-24h}$  was calculated from the predicted "liposomal AmB" and "released AmB" plasma concentration profiles.

### **2.8. PBPK-PD model for the pharmacological activity of AmB against *Candida albicans***

The effect of AmB on *Candida albicans* (*C. albicans*) was investigated in order to develop a PBPK-PD model: i. for a patient population receiving Ambisome® with a reduced albumin plasma concentration (hypalbuminaemia: albumin < 25 mg/mL), and ii. for a healthy population receiving Ambisome® with normal concentration of albumin (~4.0% w/v).

### 2.8.1. Quantification of *C. albicans*

The culture and quantification of *C. albicans* was described previously [25]. A single colony culture was started in a tube with 5 mL of SBD broth and incubated overnight at 37°C in a shaking incubator; the optical density was measured at 600 nm (OD<sub>600</sub>). The colony forming units (CFU) were determined by preparing serial dilutions and the suspensions were plated on SBD agar plates, incubated overnight at 37°C and the number of colonies were counted and related to the OD<sub>600</sub> of the culture.

### 2.8.2. Time killing experiments

Time killing experiments were performed with 10<sup>5</sup> CFU/mL of *C. albicans* using different AmB final concentrations (0.00, 0.75, 1.50 and 3.00 µg/mL) in the presence of BSA 2.0% and 4.0% w/v in KRB [an experiment without AmB was performed in order to obtain the  $k_{growth}$  of the fungal cells]. The % CFUs remaining at each time point were used for curve fitting to the exponential decay equation to obtain the killing rate coefficient for each concentration tested (Eq 6).

$$\%CFU = \%CFU_{max} * e^{-k_{kill}t} \text{ Eq 6.}$$

where %CFU is the %CFU at time  $t$ , %CFU<sub>max</sub> is the maximum %CFU,  $k_{kill}$  is the time killing rate coefficient and  $t$  is time.

A linear relation was found between  $k_{kill}$  and AmB concentration and it was used in the PBPK-PD model.

### 2.8.3 PBPK-PD modeling

The workflow for the development of the PBPK-PD model is shown in Figure 2.

To simulate a hypoalbuminaemic patient population, the protein content was halved in the validated PBPK model for the healthy subjects and the rest of the parameters remained unchanged. The "released AmB" concentration was used to calculate the  $k_{kill}$  for the 24 h time course to simulate the "released AmB" activity against *C. albicans* which was set at a concentration of  $10^5$  CFU/mL at time zero. The *C. albicans* growth rate constant ( $k_{growth}$ ) was obtained from the control time killing experiment (0.00 µg/mL AmB) by fitting the data to an exponential growth equation (Eq 7)

$$\%CFU = Ae^{k_{growth}t} \text{ (Eq 7)}$$

where %CFU is the %CFU at time t, A is the starting CFU value,  $k_{growth}$  is the growth rate constant and t is time.

### 2.9. Statistical analysis

The statistical analysis was described previously [23]. Pareto charts, based on the DoE analysis, were performed for the identification of significant effects from the *in vitro* release tests. A factor was significant when the standardized effect (bars) was larger than the line for statistical significance level ( $\alpha = 0.05$ ) (vertical line). An independent means t – test was performed to compare 2 independent means: in the AFM studies, size and surface roughness were compared against the control sample. A  $p < 0.05$  was considered statistically significant. Due to the lack of individual observed data of plasma concentration profiles, the *in vitro*  $k_{rel}$  were input into the PBPK model to obtain simulated  $AUC_{0-24h}$  which were compared against the  $AUC_{0-24h}$  obtained from the simulated data generated by the validated PBPK model.



Additionally, the 90% confidence interval (90% CI) for the ratio of the geometric means of the simulated  $AUC_{0-24h}$  obtained with the *in vitro*  $k_{rel}$  and the  $AUC_{0-24h}$  obtained from the simulated data generated by the validated PBPK model were calculated. As recommended by the FDA guidance, both "liposomal AmB" and "released AmB" were evaluated [39]. Data analysis, creation and analysis of DoE were performed with the statistical software Statgraphics Centurion XVII (USA) and the 90% CI were calculated with IBM SPSS Statistics 25 (USA).

### 3. Results and discussion

#### 3.1. *In vitro* release testing of Ambisome®

*In vitro* release profiles of AmB from Ambisome® in both hydrodynamic setups are shown in Figure 3 and parameters obtained after fitting to the first order equation model are presented in Table 4.

For the sample and separate setup, the statistical analysis (Figure 4a) showed that the buffer was a significant factor affecting  $\%AmB_{released}max$  with a higher release in KRB, the presence of BSA 4.0% w/v had a significant negative effect. The interaction between buffer and BSA was significant as the amount released in KRB with BSA is slightly higher than in PBS with BSA, while in media without BSA there is no difference. The release rate constant was affected in the same way as  $\%AmB_{released}max$  but the interaction between buffer and BSA showed that the release rate is faster in KRB than in PBS without BSA and there is not a statistical significant difference in KRB and PBS with BSA. For the continuous flow setup (Figure 4b), the flow rate was the only significant factor affecting AmB release from the liposomes, with a positive effect on the  $AUC_{0-12h}$ .

#### 3.2. AFM studies

Figure 5 shows the images obtained from the AFM and Table 5 contains the parameters of the liposome characteristics measured by AFM.

Diameter of the liposomal structures in samples from KRB BS 20.0 mM PL 4.0 mM are significantly higher than the control sample; liposomes could be merging with each other or the inclusion of BS PL could alter the structure of the liposome resulting in a higher size before the disruption. Liposomes were not visible in the sample of from KRB BS 20.0 mM PL 4.0 mM BSA 4.0% w/v, probably due to the incubation period of this sample.

### 3.3. PBPK modeling of Ambisome® administered to healthy subjects

The simulated plasma concentration profiles obtained with the validated PBPK model for the administration of Ambisome® to healthy subjects are shown in Figure 6.

Using the parameter identification method, the optimal values for the parameters investigated were:  $k_{rel-iv} = 0.60 \text{ h}^{-1}$ ,  $\log P$  (released AmB) = 3.24,  $\log P$  (liposomal AmB) = 1.0, Specific clearance for the immune removal "enzyme" =  $2.57 \text{ h}^{-1}$  and AAG1  $k_{diss} = 0.42 \text{ } \mu\text{mol/L}$ . The  $\log P$  and  $\text{clog} P$  values reported in the literature, are between -2.33 to 2.14 (Table 2) providing a wide interval for the true value. The value obtained from parameter identification fitting was 3.24 which could be supported considering the distribution of the values previously reported (Table 2).

The PBPK model described closely the average observed data for "liposomal AmB" and "released AmB" ( $\% .AUC_{0-24h} \text{ predicted} / AUC_{0-24h} \text{ observed}$  were 94% and 101%, respectively). Comparing the developed PBPK model in this study with the one reported by Kagan et al [21], the main difference was the  $k_{rel-iv}$  from this model was faster:  $0.60 \text{ h}^{-1} > 0.0035 \text{ h}^{-1}$  [21] and there was no initial rapid release of 8.0% of the dose, as was included by Kagan et al [21]. It could be due to simulated AmB release taking place in all of the

compartments in the model presented by Kagan et al. [21], while in this study; the release was only in plasma.

The sensitivity analysis is shown in Figure 7. Parameters such as aqueous solubility ("liposomal AmB" and "released AmB"), solute radius ("liposomal AmB"), specific biliary clearance ("liposomal AmB" and "released AmB"),  $k_{diss}$  for AAG1 and APOB ("released AmB"), and the GFR for "released AmB" did not have a significant impact on the  $AUC_{0-24h}$  of "liposomal AmB" or "released AmB". For the "liposomal AmB", the fraction unbound to proteins had the greatest impact on the model. It can be observed how the "liposomal AmB" in plasma decreases as the fraction unbound increases, leading to a decrease in "released AmB", as there will be less "liposomal AmB" available in plasma to release drug.  $k_{rel-iv}$  had a high impact on both "liposomal AmB" and "released AmB" (Figure 7), with a higher release rate constant leading to an increase in the "released AmB" and a decrease in the "liposomal AmB". For "released AmB", logP is the factor with the highest effect on  $AUC_{0-24h}$ .

#### 3.4. Evaluation of the *in vitro* release profiles using the PBPK model

The predictability of the *in vitro* release tests is presented in Figure 8 for both "liposomal AmB" and "released AmB".

For the "liposomal AmB", the  $AUC_{0-24h}$  obtained with the *in vitro*  $k_{rel}$  where BSA was present in the media were similar to the  $AUC_{0-24h}$  obtained from the validated PBPK model, regardless of the type of the buffer or the hydrodynamic conditions. The  $AUC_{0-24h}$  values were only similar for a medium without BSA in the low velocity setup (Figure 8). For the "released AmB", the  $AUC_{0-24h}$  obtained with the *in vitro*  $k_{rel}$  in media with BSA were close to attaining similarity to the *in vivo* profiles, as all the tests (except KRB BS PL BSA low agitation) revealed one extreme of the 90% CI between 80 – 125%. It can be noticed that the tests performed with the continuous flow setup under-predicted the plasma concentration of the

"released AmB". An increasing flow rate leads to a higher drug release (Figure 4) thus further exploration of flow rate effect could be conducted to identify the flow rate resulting in release profiles suitable for simulation of *in vivo* release. The  $AUC_{0-24h}$  could not be calculated for the high velocity profiles as for the medium without BSA the standard deviation was higher than the mean and for the medium with BSA the profiles could not be fitted to the first order equation. The model developed is suitable for the evaluation of the *in vitro* release tests and could support the development of a biopredictive *in vitro* release test. It has to be noted that for the prediction of the plasma concentration of "liposomal AmB" and "released AmB", the presence of BSA was a critical factor, thus, information on the exact mechanism of the protein binding to the liposomes could further improve the model developed. Furthermore, the accuracy of model could be further improved through inclusion of parameters capturing AmB binding to red blood cells, as in general only plasma concentrations are presented in the literature while the formulation is obviously administered to the venous blood pool.

### 3.5. PBPK – PD modeling for the patient (hypoalbuminaemic) population.

Parameters obtained after fitting to the exponential decay equation model for the time killing experiments are presented in Table 6. A linear relationship between the AmB concentration and the time killing rate coefficient was found for experiments with BSA 2.0 and 4.0% w/v, (Eq 8 and eq. 9, respectively)

$$\text{time killing rate coefficient } (h^{-1}) = 0.1923(mL * h^{-1}) / \mu g + 0.2102 h^{-1} \quad \text{Eq 8.}$$

$$\text{time killing rate coefficient } (h^{-1}) = 0.1167 (mL * h^{-1}) / \mu g + 0.014 h^{-1} \quad \text{Eq 9.}$$

The simulated plasma concentration profiles for "liposomal AmB" and "released AmB" in the extrapolated hypoalbuminaemic population and the healthy subject population are presented in Figure 9a. It can be observed that both "liposomal AmB" and "released AmB" are at a lower concentration as a consequence of the decrease of the amount of proteins present. There is a

441 lower concentration as with more unbound drug there is more drug available for distribution  
442 and clearance. Figure 9b shows the simulated plasma concentration profiles for a typical  
443 administration of Ambisome® to a patient with a systemic fungal infection (300 mg, infusion  
444 4 h) in the simulated hypoalbuminaemic patient and in a subject with normal albumin levels.

445 Equations 8 and 9 were used in the PBPK-PD model to simulate the killing of *C. albicans*  
446 (Figure 9c). It can be observed how the growth of the fungal cells is reduced by the  
447 administration of Ambisome® (Figure 9d) with a higher effect in the simulated  
448 hypoalbuminaemic patient than in the subject with normal albumin levels. From the time  
449 killing studies and previous data on minimum inhibitory and fungicidal concentrations [25], a  
450 higher fungicidal effect is reached with a lower AmB concentration in the presence of BSA  
451 2.0% w/v as there is more unbound drug able to exert its pharmacological effect. It has to be  
452 noted that only the effect of released AmB is evaluated in this PBPK-PD model. The humoral  
453 and cellular immune responses and the effect that the liposomal AmB could have on *C.*  
454 *albicans* are not considered, nor is the effect of fungal phospholipases on liposomal integrity  
455 and AmB release. A number of  $10^5$  CFU/mL were used to simulate the effect of AmB *in vivo*  
456 as this was the concentration of the fungal cell suspensions used in the time killing experiments.

457 It has been reported that a concentration of 100 – 1000 CFU/mL are found in cultures of blood  
458 from patients with systemic fungal infection [41, 42]. The PBPK-PD analysis could be further  
459 improved by using the adequate number of CFU quantified in plasma from infected patients to  
460 evaluate the response of the humoral immune response and not only the effect of the protein  
461 content. In plasma from healthy subjects the fungal cells did not grow (data not shown), thus,  
462 the results of the PBPK-PD model for the healthy subject must be only considered as an  
463 exercise for comparative purposes. For this model, only the changes in the albumin levels were  
464 considered, leaving aside the physiological characteristics of septic or critically ill patients. In  
465 order to improve the model, the change in the activity of the immune enzyme should be

adjusted to the patient population as the immune system might be compromised or activated, and the  $k_{rel-iv}$ , which the *in vitro* tests showed to be dependent on the albumin concentration, should also be adjusted. This approach reveals the potential of the use of *in vitro* release data and suitable microbiology data in combination with a PBPK-PD model in order to guide parenteral formulation development based on pharmacodynamics and therapeutic outcomes.

#### 4. Conclusions

The literature available for *in vitro* release testing of controlled release parenteral formulations is limited. The evaluation of factors that can affect the release from these formulations and the development of *in vitro* release tests that are able to predict the *in vivo* performance are of high importance. In this work, the development of a clinically relevant *in vitro* release test for the liposomal formulation of AmB (Ambisome®) was investigated. A PBPK model was developed for the administration of Ambisome® to healthy subjects, which was used to identify the critical factors for AmB release from liposomes and the *in vivo* predictability of the *in vitro* release tests. The presence of BSA in the media was the most critical factor affecting the AmB release, and the *in vitro* release profiles from tests with BSA in the medium were biopredictive. Successful predictions of the “liposomal AmB” and the “released AmB” plasma concentration profile were obtained with both hydrodynamic setups tested (sample and separate method and continuous flow method). A PBPK-PD model of the activity of AmB on fungal cells was developed based on the predicted “released AmB” plasma concentration profile in a hypoalbuminaemic population in order to illustrate the potential of linking *in vitro* release testing, PBPK modeling and microbiology data.

#### Acknowledgments

489 Part of this work has been previously presented at the AAPS PharmSci 360 annual meeting in  
490 Washington, DC November 2018 (poster presentation). The authors would like to thank the  
491 Mexican Council of Science and Technology (CONACyT) for the PhD scholarship of Dr R  
492 Diaz de Leon-Ortega, Dr Wei-Feng Xue (University of Kent, UK) for his help with the AFM  
493 studies, Dr Albert Bolhuis for his help with the microbiology studies and Dr Andrea Edginton  
494 (University of Waterloo, Canada) for her help with PK-Sim<sup>®</sup> software.

495

## 5. References

- [1] A. Abend, T. Heimbach, M. Cohen, F. Kesisoglou, X. Pepin, S. Suarez-Sharp, Dissolution and Translational Modeling Strategies Enabling Patient-Centric Drug Product Development: the M-CERSI Workshop Summary Report, *The AAPS Journal*, 20 (2018) 60.
- [2] P. Espié, D. Tytgat, M.-L. Sargentini-Maier, I. Poggesi, J.-B. Watelet, Physiologically based pharmacokinetics (PBPK), *Drug Metabolism Reviews*, 41 (2009) 391-407.
- [3] F. Khalil, S. Laer, Physiologically based pharmacokinetic modeling: methodology, applications, and limitations with a focus on its role in pediatric drug development, *Journal of biomedicine & biotechnology*, 2011 (2011) 907461.
- [4] H.M. Jones, I.B. Gardner, K.J. Watson, Modelling and PBPK Simulation in Drug Discovery, *The AAPS Journal*, 11 (2009) 155-166.
- [5] H.K. Batchelor, N. Fotaki, S. Klein, Paediatric oral biopharmaceutics: key considerations and current challenges, *Advanced drug delivery reviews*, 73 (2014) 102-126.
- [6] F. Kesisoglou, J. Chung, J. van Asperen, T. Heimbach, Physiologically Based Absorption Modeling to Impact Biopharmaceutics and Formulation Strategies in Drug Development- Industry Case Studies, *Journal of pharmaceutical sciences*, 105 (2016) 2723-2734.
- [7] X. Zhuang, C. Lu, PBPK modeling and simulation in drug research and development, *Acta Pharmaceutica Sinica B*, 6 (2016) 430-440.
- [8] FDA, 2018. Physiologically Based Pharmacokinetic Analyses — Format and Content. Available from: <https://www.fda.gov/downloads/Drugs/GuidanceComplianceRegulatoryInformation/Guidances/UCM531207.pdf>. Access date: 31/07/2019.
- [9] EMA, Guideline on the qualification and reporting of physiologically based pharmacokinetic (PBPK) modelling and simulation, 2016. Available from: <https://www.ema.europa.eu/documents/scientific-guideline/guideline-qualification-reporting->



521 physiologically-based-pharmacokinetic-pbpbk-modelling-simulation\_en.pdf. Access date:  
 522 31/07/2019.

523 [10] X.Y. Zhang, M.N. Trame, L.J. Lesko, S. Schmidt, Sobol Sensitivity Analysis: A Tool to  
 524 Guide the Development and Evaluation of Systems Pharmacology Models, CPT:  
 525 pharmacometrics & systems pharmacology, 4 (2015) 69-79.

526 [11] K. McNally, R. Cotton, G.D. Loizou, A Workflow for Global Sensitivity Analysis of  
 527 PBPK Models, Frontiers in pharmacology, 2 (2011) 31.

528 [12] M. Ulldemolins, J.A. Roberts, J. Rello, D.L. Paterson, J. Lipman, The effects of  
 529 hypoalbuminaemia on optimizing antibacterial dosing in critically ill patients, Clinical  
 530 Pharmacokinetics, 50 (2011) 99-110.

531 [13] L. Kuepfer, C. Niederalt, T. Wendl, J.F. Schlender, S. Willmann, J. Lippert, M. Block, T.  
 532 Eissing, D. Teutonico, Applied Concepts in PBPK Modeling: How to Build a PBPK/PD Model,  
 533 CPT: pharmacometrics & systems pharmacology, 5 (2016) 516-531.

534 [14] K. Chen, S. Teo, K.Y. Seng, Sensitivity analysis on a physiologically-based  
 535 pharmacokinetic and pharmacodynamic model for diisopropylfluorophosphate-induced  
 536 toxicity in mice and rats, Toxicology mechanisms and methods, 19 (2009) 486-497.

537 [15] E. Asin-Prieto, A. Rodriguez-Gascon, A. Isla, Applications of the  
 538 pharmacokinetic/pharmacodynamic (PK/PD) analysis of antimicrobial agents, Journal of  
 539 infection and chemotherapy : official journal of the Japan Society of Chemotherapy, 21 (2015)  
 540 319-329.

541 [16] E.I. Nielsen, O. Cars, L.E. Friberg, Pharmacokinetic/pharmacodynamic (PK/PD) indices  
 542 of antibiotics predicted by a semimechanistic PKPD model: a step toward model-based dose  
 543 optimization, Antimicrobial agents and chemotherapy, 55 (2011) 4619-4630.

544 [17] M.W. Sadiq, E.I. Nielsen, D. Khachman, J.M. Conil, B. Georges, G. Houin, C.M. Laffont,  
 545 M.O. Karlsson, L.E. Friberg, A whole-body physiologically based pharmacokinetic (WB-

546 PBPK) model of ciprofloxacin: a step towards predicting bacterial killing at sites of infection,  
 547 *Journal of pharmacokinetics and pharmacodynamics*, 44 (2017) 69-79.

548 [18] J. Mora-Duarte, R. Betts, C. Rotstein, A.L. Colombo, L. Thompson-Moya, J. Smietana,  
 549 R. Lupinacci, C. Sable, N. Kartsonis, J. Perfect, Comparison of caspofungin and amphotericin  
 550 B for invasive candidiasis, *The New England journal of medicine*, 347 (2002) 2020-2029.

551 [19] E.M. Johnson, J.O. Ojwang, A. Szekely, T.L. Wallace, D.W. Warnock, Comparison of In  
 552 Vitro Antifungal Activities of Free and Liposome-Encapsulated Nystatin with Those of Four  
 553 Amphotericin B Formulations, *Antimicrob. Agents. Chemother.*, 42 (1998) 1412-1416.

554 [20] L. Kagan, P. Gershkovich, K.M. Wasan, D.E. Mager, Physiologically Based  
 555 Pharmacokinetic Model of Amphotericin B Disposition in Rats Following Administration of  
 556 Deoxycholate Formulation (Fungizone®): Pooled Analysis of Published Data, *The AAPS*  
 557 *Journal*, 13 (2011) 255.

558 [21] L. Kagan, P. Gershkovich, K.M. Wasan, D.E. Mager, Dual Physiologically Based  
 559 Pharmacokinetic Model of Liposomal and Nonliposomal Amphotericin B Disposition,  
 560 *Pharmaceutical Research*, 31 (2014) 35-45.

561 [22] R. Díaz de León–Ortega, D.M. D'Arcy, N. Fotaki, Investigating Factors That Affect In  
 562 vitro Drug Release From A Parenteral Liposomal Formulation, in: *AAPS*, Washington DC,  
 563 USA, 2018.

564 [23] R. Diaz de Leon-Ortega, D.M. D'Arcy, D.L. Lamprou, W.F. Xue, N. Fotaki, In vitro in  
 565 vivo relations for the parenteral liposomal formulation of Amphotericin B. Part 1: A  
 566 biorelevant and clinically relevant approach, Submitted to the *Journal of Controlled Release*,  
 567 (2019).

568 [24] P. Egger, R. Bellmann, C.J. Wiedermann, Determination of amphotericin B, liposomal  
 569 amphotericin B, and amphotericin B colloidal dispersion in plasma by high-performance liquid  
 570 chromatography, *J. Chromatogr. B: Anal. Technol. Biomed. Life Sci.*, 760 (2001) 307-313.

571 [25] R. Diaz de Leon-Ortega, D.M. D'Arcy, A. Bolhuis, N. Fotaki, Investigation and simulation  
572 of dissolution with concurrent degradation under healthy and hypoalbuminaemic simulated  
573 parenteral conditions- case example Amphotericin B, European journal of pharmaceutics and  
574 biopharmaceutics : official journal of Arbeitsgemeinschaft fur Pharmazeutische  
575 Verfahrenstechnik e.V, (2018).

576 [26] N. Fotaki, Flow-through cell apparatus (USP apparatus 4): Operation and features,  
577 Dissolution Technol, 18 (2011) 46-49.

578 [27] I. Bekersky, R.M. Fielding, D.E. Dressler, J.W. Lee, D.N. Buell, T.J. Walsh,  
579 Pharmacokinetics, Excretion, and Mass Balance of Liposomal Amphotericin B (AmBisome)  
580 and Amphotericin B Deoxycholate in Humans, Antimicrobial Agents and Chemotherapy, 46  
581 (2002) 828-833.

582 [28] I. Bekersky, R.M. Fielding, D.E. Dressler, J.W. Lee, D.N. Buell, T.J. Walsh, Plasma  
583 protein binding of amphotericin B and pharmacokinetics of bound versus unbound  
584 amphotericin B after administration of intravenous liposomal amphotericin B (AmBisome) and  
585 amphotericin B deoxycholate, Antimicrob. Agents. Chemother., 46 (2002) 834-840.

586 [29] DrugBank, Amphotericin B, 2005. Available from:  
587 <https://www.drugbank.ca/drugs/DB00681>. Access date: 31/07/2019

588 [30] Sigma-Aldrich, Amphotericin B, 2015. Available from:  
589 [https://www.sigmaaldrich.com/content/dam/sigma-](https://www.sigmaaldrich.com/content/dam/sigma-aldrich/docs/Sigma/Datasheet/6/a9528dat.pdf)  
590 [aldrich/docs/Sigma/Datasheet/6/a9528dat.pdf](https://www.sigmaaldrich.com/content/dam/sigma-aldrich/docs/Sigma/Datasheet/6/a9528dat.pdf). Access date: 31/07/2019

591 [31] S.S. Bharate, V. Kumar, R.A. Vishwakarma, Determining Partition Coefficient (Log P),  
592 Distribution Coefficient (Log D) and Ionization Constant (pKa) in Early Drug Discovery,  
593 Combinatorial chemistry & high throughput screening, 19 (2016) 461-469.

594 [32] ChemSpider, Amphotericin B, 2015. Available from:  
595 <http://www.chemspider.com/Chemical-Structure.10237579.html>. Access date: 31/07/2019

596 [33] M.T. Lamy-Freund, V.F. Ferreira, S. Schreier, Polydispersity of aggregates formed by the  
 597 polyene antibiotic amphotericin B and deoxycholate. A spin label study, *Biochim. Biophys.*  
 598 *Acta, Biomembr.*, 981 (1989) 207-212.

599 [34] J. Mazerski, J. Grzybowska, E. Borowski, Influence of net charge on the aggregation and  
 600 solubility behaviour of amphotericin B and its derivatives in aqueous media, *European*  
 601 *biophysics journal*, 18 (1990) 159-164.

602 [35] J. Barwicz, S. Christian, I. Gruda, Effects of the aggregation state of amphotericin B on  
 603 its toxicity to mice, *Antimicrob. Agents. Chemother.*, 36 (1992) 2310-2315.

604 [36] Y. Ridente, J. Aubard, J. Bolard, Absence in amphotericin B-spiked human plasma of the  
 605 free monomeric drug, as detected by SERS, *FEBS letters*, 446 (1999) 283-286.

606 [37] Gilead, Ambisome®,  
 607 [http://www.gilead.com/~media/files/pdfs/medicines/other/ambisome/ambisome\\_pi.pdf?la=en](http://www.gilead.com/~media/files/pdfs/medicines/other/ambisome/ambisome_pi.pdf?la=en)  
 608 n, (2015).

609 [38] Y. Yokouchi, T. Tsunoda, T. Imura, H. Yamauchi, S. Yokoyama, H. Sakai, M. Abe, Effect  
 610 of adsorption of bovine serum albumin on liposomal membrane characteristics, *Colloids and*  
 611 *Surfaces B: Biointerfaces*, 20 (2001) 95-103.

612 [39] T. Hernández-Caselles, J. Villalaín, J.C. Gómez-Fernández, Influence of liposome charge  
 613 and composition on their interaction with human blood serum proteins, *Molecular and Cellular*  
 614 *Biochemistry*, 120 (1993) 119-126.

615 [40] S.L. Law, W.Y. Lo, S.H. Pai, G.W. Teh, F.Y. Kou, The adsorption of bovine serum  
 616 albumin by liposomes, *International Journal of Pharmaceutics*, 32 (1986) 237-241.

617 [41] B. Misme-Aucouturier, M. Albassier, N. Alvarez-Rueda, P. Le Pape, Specific Human and  
 618 *Candida* Cellular Interactions Lead to Controlled or Persistent Infection Outcomes during  
 619 Granuloma-Like Formation, *Infection and Immunity*, 85 (2017) e00807-00816.

620 [42] C.D. Pfeiffer, G.P. Samsa, W.A. Schell, L.B. Reller, J.R. Perfect, B.D. Alexander,  
621 Quantitation of Candida CFU in Initial Positive Blood Cultures, Journal of Clinical  
622 Microbiology, 49 (2011) 2879-2883.

623

624 **Tables**

625 **Table 1.** Levels and factors investigated with the sample and separate setup for the release  
 626 studies of AmB from Ambisome® in clinically relevant media.

Level	BSA %w/v	Medium	Agitation (rpm)
- 1	2.0	PBS BS 19.8 mM PL 7.9 mM	130 (Low Agitation)
+ 1	4.0	KRB BS 20.0 mM PL 4.0 mM	380 (High Agitation)

627

**Table 2.** PK-Sim model set up: physicochemical properties, distribution and clearance parameters of "released AmB" and "liposomal AmB" (Ambisome<sup>®</sup>) after administration to healthy subjects.

<b>"Released AmB"</b>	
<b>Molecular weight (g/mol)</b>	924 [29, 30]
<b>log P</b>	0.80 [29], 0.94 [31], 1.84 [31], 2.14 [31]
<b>clog P</b>	- 2.33 [29], - 0.66 [29], 1.16 [32]
<b>pka</b>	acidic 5.5 [30], basic 10.0 [30]
<b>Solubility at pH = 7</b>	0.09 µg/mL [33], 1.38 µg/mL [34], 6.00 µg/mL [35]
<b>fraction unbound (albumin)</b>	0.05 [28]
<b>Distribution volume</b>	2340 ± 202 mL/kg [27]
<b>Cl<sub>renal</sub></b>	0.07 ± 0.01 mL/min/kg [27]. GFR fraction = 0.875
<b>Cl<sub>biliary</sub></b>	0.09 ± 0.02 mL/min/kg [27]. k <sub>bil</sub> = 0.002 h <sup>-1</sup>

<b>Binding partners</b>	alfa 1 acid glycoprotein (AAG1), EST expression, $k_{\text{diss}} = 1.07 - 2.44 \mu\text{mol/L}$ (approximation from unbound fraction) [27]
	beta lipoprotein (APOB), EST expression, $k_{\text{diss}} = 0.25 \mu\text{mol/L}$ [36]
<b>"Liposomal AmB"</b>	
<b>Distribution volume</b>	$1628 \pm 876 \text{ mL/kg}$ [27]
<b>Cl renal</b>	$0.01 \pm 0.00 \text{ mL/min/kg}$ [27], GFR fraction = 0.125
<b>Cl biliary</b>	$0.01 \pm 0.00 \text{ mL/min/kg}$ [27], $k_{\text{bil}} = 0.0003 \text{ h}^{-1}$
<b>Assumptions for the model, considering the "liposomal AmB" as a molecule</b>	
<b>Molecular weight (g/mol)</b>	924
<b>Radius (solute)</b>	80 nm [37]
<b>log P</b>	Parameter to identify, starting value 0.8
<b>pka</b>	Neutral



<b>Solubility at pH = 7</b>	290 mg/mL [calculated from the total amount of powder in a formulation vial (14.5 g), dissolved in 50 mL of water]								
<b>fraction unbound albumin</b>	0.05								
<b>Immune removal</b>	<p>Metabolizing enzymes -&gt; Intrinsic clearance First order -&gt;</p> <p>Relative expression -&gt; Intracellular -&gt; Endosomal</p> <table> <tr> <td>Plasma</td><td>100%</td></tr> <tr> <td>Liver periportal</td><td>100%</td></tr> <tr> <td>Liver pericentral</td><td>100%</td></tr> <tr> <td>Spleen</td><td>100%</td></tr> </table>	Plasma	100%	Liver periportal	100%	Liver pericentral	100%	Spleen	100%
Plasma	100%								
Liver periportal	100%								
Liver pericentral	100%								
Spleen	100%								

**Table 3.** Parameters and the range in which the parameters were investigated in the sensitivity analysis of the validated PBPK model of Ambisome® administration.

Parameter	Abbreviation	Interval tested
log P ("liposomal AmB")	logP (lip)	0 – 2 (log units)
log P ("released AmB")	logP (rel)	2.24 – 4.24 (log units)
Aqueous solubility ("liposomal AmB")	Sol (lip)	90 – 490 (µg/mL)
Aqueous solubility ("released AmB")	Sol (rel)	0.01 – 6.00 (µg/mL)
Radius solute ("liposomal AmB")	Rad (lip)	40 – 120 (nm)
$k_{bil}$ ("liposomal AmB")	Bil (lip)	0.0001 – 0.0005 ( $h^{-1}$ )
$k_{bil}$ ("released AmB")	Bil (rel)	0.001 – 0.003 ( $h^{-1}$ )
GFR ("liposomal AmB")	GFR (lip)	0 – 1 (fraction)
GFR ("released AmB")	GFR (rel)	0 – 1 (fraction)
"Immune enzyme" specific clearance	Imm	1.57 – 3.57 ( $h^{-1}$ )
APOB1 $k_{diss}$	APOB1	0.12 – 0.37 (µmol/L)
AAG1 $k_{diss}$	AAG1	0.21 – 0.63 (µmol/L)
$k_{rel-iv}$	krel	0.114 - 3.539 ( $h^{-1}$ )
Unbound fraction ("liposomal AmB")	fU (lip)	0.05 – 0.95 (fraction)

Unbound fraction ("released AmB")	fU (rel)	0.05 – 0.95 (fraction)
-----------------------------------	----------	------------------------

**Table 4.** Parameters obtained after fitting (Eq 3) of %AmB released profiles from Ambisome® with the sample and separate setup and the continuous flow setup [LA: low agitation, HA: high agitation, LV: low velocity, HV: high velocity] (Mean  $\pm$  SD, n = 3).

Buffer	BSA (%w/v)	Surfactant concentrations	Agitation/velocity	$k_{rel}$ (h <sup>-1</sup> )	% <i>AmB</i> <sub>released</sub> <i>max</i>
Sample and separate					
PBS	0.0	BS 19.8 mM PL 7.9 mM	LA	1.425 $\pm$ 0.101	96.258 $\pm$ 0.101
PBS	4.0	BS 19.8 mM PL 7.9 mM	LA	0.701 $\pm$ 0.060	78.573 $\pm$ 2.548
KRB	0.0	BS 20.0 mM PL 4.0 mM	LA	3.034 $\pm$ 0.106	99.201 $\pm$ 0.321
KRB	4.0	BS 20.0 mM PL 4.0 mM	LA	0.621 $\pm$ 0.192	81.662 $\pm$ 2.931
PBS	0.0	BS 19.8 mM PL 7.9 mM	HA	2.437 $\pm$ 0.129	98.953 $\pm$ 0.158
PBS	4.0	BS 19.8 mM PL 7.9 mM	HA	0.410 $\pm$ 0.052	73.031 $\pm$ 6.013
KRB	0.0	BS 20.0 mM PL 4.0 mM	HA	2.747 $\pm$ 0.046	99.146 $\pm$ 0.072

KRB	4.0	BS 20.0 mM PL 4.0 mM	HA	$0.896 \pm 0.041$	$88.141 \pm 2.480$
Continuous flow					
KRB	0.0	BS 20.0 mM PL 4.0 mM	LV	$0.305 \pm 0.071$	$49.181 \pm 17.119$
KRB	4.0	BS 20.0 mM PL 4.0 mM	LV	$0.467 \pm 0.162$	$43.101 \pm 10.563$
KRB	0.0	BS 20.0 mM PL 4.0 mM	HV	$1.364 \pm 1.890$	$60.416 \pm 4.593$
KRB	4.0	BS 20.0 mM PL 4.0 mM	HV	-	-

**Table 5.** Properties of liposomes obtained from atomic force microscopy from the samples prepared in media with BS PL in the presence and absence of BSA. Mean  $\pm$  SD. n = 20 Random Particles.

Sample	Diameter (nm)	Surface Roughness (nm)	Density ( $\mu\text{m}^{-2}$ )
KRB control (centrifugation/vacuum)	69.4 $\pm$ 18.9	12.9 $\pm$ 1.6	11.9
KRB BS 20.0 mM PL 4.0 mM	130.0 $\pm$ 13.0	10.1 $\pm$ 2.7	7.7
KRB BS 20.0 mM PL 4.0 mM BSA 4.0% w/v	No Particles		

**Table 6.** Parameters obtained after fitting (Equation 6) of CFU time profiles from time killing experiments in KRB BSA 2 and 4% w/v using different concentrations of AmB (0.75, 1.5 and 3.0  $\mu\text{g/mL}$ ) (Mean  $\pm$  SD, n = 2).

BSA (%w/v)	AmB ( $\mu\text{g/mL}$ )	% $CFU_{max}$	$k_{kill}$ ( $\text{h}^{-1}$ )	$R^2$	AIC
2.0	0.75	105.1 $\pm$ 5.23	0.33 $\pm$ 0.03	0.86 $\pm$ 0.02	52.88 $\pm$ 0.3
	1.50	110.65 $\pm$ 4.17	0.54 $\pm$ 0.03	0.93 $\pm$ 0.05	47.16 $\pm$ 6.17
	3.00	110.6 $\pm$ 5.37	0.77 $\pm$ 0.11	0.92 $\pm$ 0.05	48 $\pm$ 6.43
4.0	0.75	101.75 $\pm$ 4.6	0.11 $\pm$ 0.01	0.89 $\pm$ 0.01	47.25 $\pm$ 2.38
	1.50	123.8 $\pm$ 10.04	0.17 $\pm$ 0.03	0.84 $\pm$ 0.07	54.71 $\pm$ 5.18
	3.00	107.65 $\pm$ 6.15	0.37 $\pm$ 0.01	0.9 $\pm$ 0	50.27 $\pm$ 1.06

## Figure captions

**Figure 1.** Workflow for the PBPK modeling of "liposomal AmB" and "released AmB" after the administration of Ambisome® to healthy subjects

**Figure 2.** Workflow for the PBPK-PD modeling of the liposomal and released AmB after the administration of Ambisome® to a hypoalbuminaemic population in order to simulate the pharmacological activity of the released AmB on *C. albicans*.

**Figure 3.** % AmB released with the a) sample and separate and the b) continuous flow setup at 37 °C to investigate the effect of the type of buffer, the BSA 4.0% w/v presence and the hydrodynamics in clinically relevant media with BS – PL. (Mean  $\pm$  SD, n=3; solid lines: media with BSA 4.0% w/v; dotted lines: media without BSA 4.0% w/v).

**Figure 4.** Pareto charts for the estimated effects of the main factors and 2 level interactions of the analysis of a) % $AmB_{releasedmax}$  and  $k_{rel}$  from the sample and separate setup and b) the  $AUC_{0-12h}$  from the continuous flow method. A factor was significant when the estimated effect (horizontal bars) was larger than the standardized effect (vertical line).

**Figure 5.** AFM images to evaluate the effect of media components on Ambisome® liposomes. a) KRB BS 20.0 mM PL 4.0 mM, b) KRB BS 20.0 mM PL 4.0 mM BSA 4.0% w/v. The scale bar represents 200 nm.

**Figure 6.** Observed and simulated (PBPK model) plasma concentration profiles of "liposomal AmB" and "released AmB" after the administration of Ambisome® to healthy subjects [25, 26].

**Figure 7.** Sensitivity analysis of PBPK model parameters on the "liposomal AmB" and "released AmB"  $AUC_{0-24h}$  obtained from simulated plasma concentrations in healthy subjects. The black line is the  $AUC_{0-24h}$  obtained from the validated PBPK model for healthy subjects.

**Figure 8.**  $AUC_{0-24h}$  calculated from simulated plasma concentration profiles with with the  $k_{rel}$  from the *in vitro* release profiles against the  $AUC_{0-24h}$  obtained from the validated PBPK model for "liposomal AmB" and "released AmB". n = 5 subjects for each population.

**Figure 9.** PBPK-PD model for a hypoalbuminaemic population (plasma protein fraction 0.5; healthy subjects: plasma protein fraction 1.0) –Simulated concentration and its pharmacodynamic effect on fungal cells. a) Simulated plasma concentration profiles of "liposomal AmB" and "released AmB" from the validated PBPK model for healthy subjects and the hypothesised model for the hypoalbuminaemic population, b) simulation of plasma concentrations following administration of a 300 mg dose of Ambisome<sup>®</sup>, c) simulated time killing rate coefficient ( $k_{kill}$ ) (corresponding to the simulated plasma concentration profile of Figure 9b), and d) effect of the administration of Ambisome<sup>®</sup> on the growth of *Candida albicans*.



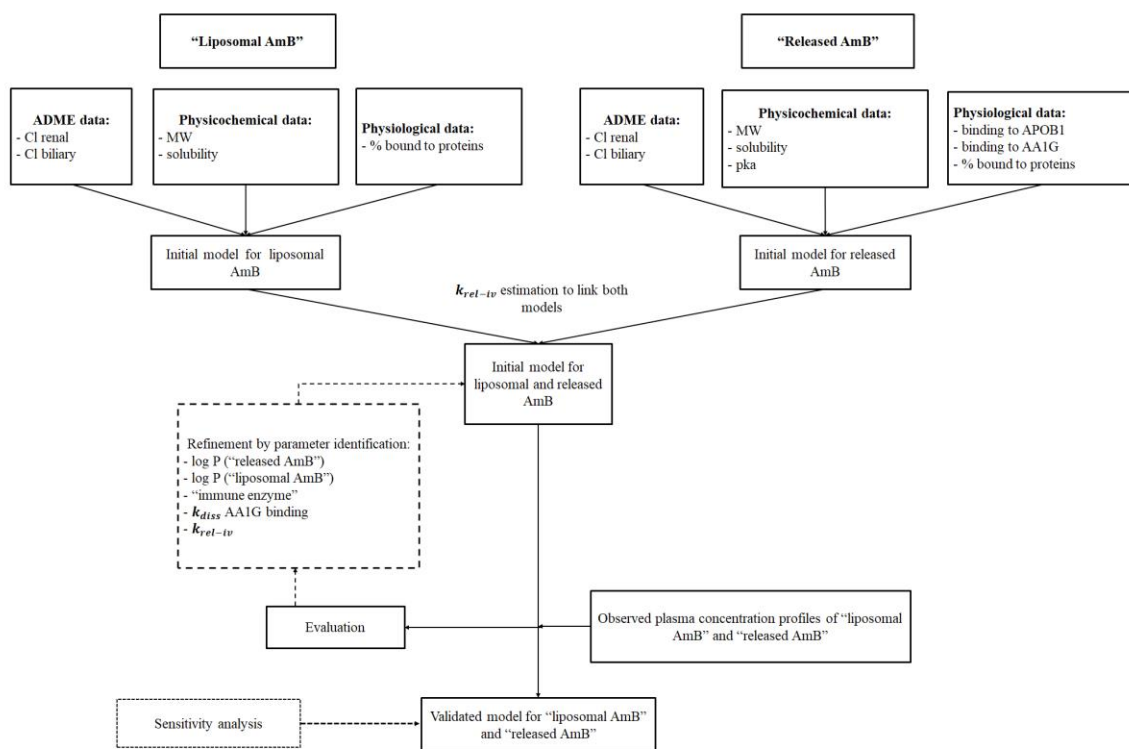


**Figure 1**

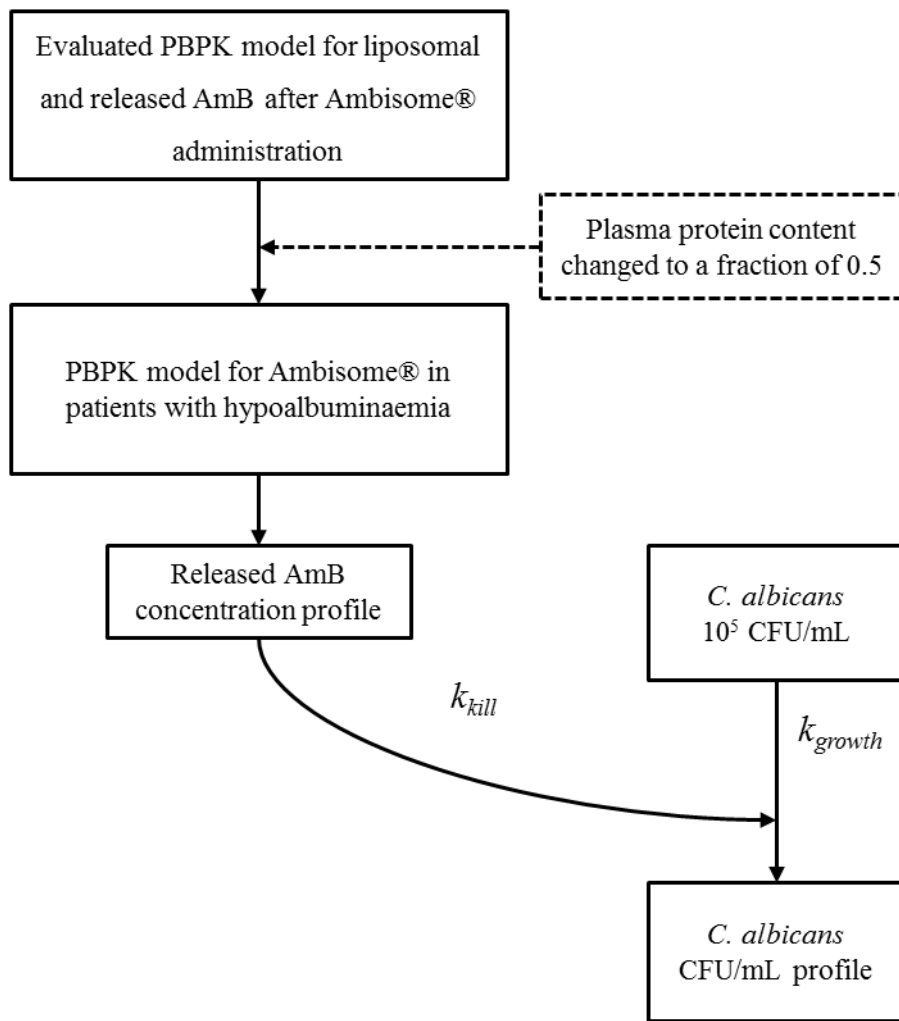


**Figure 2**

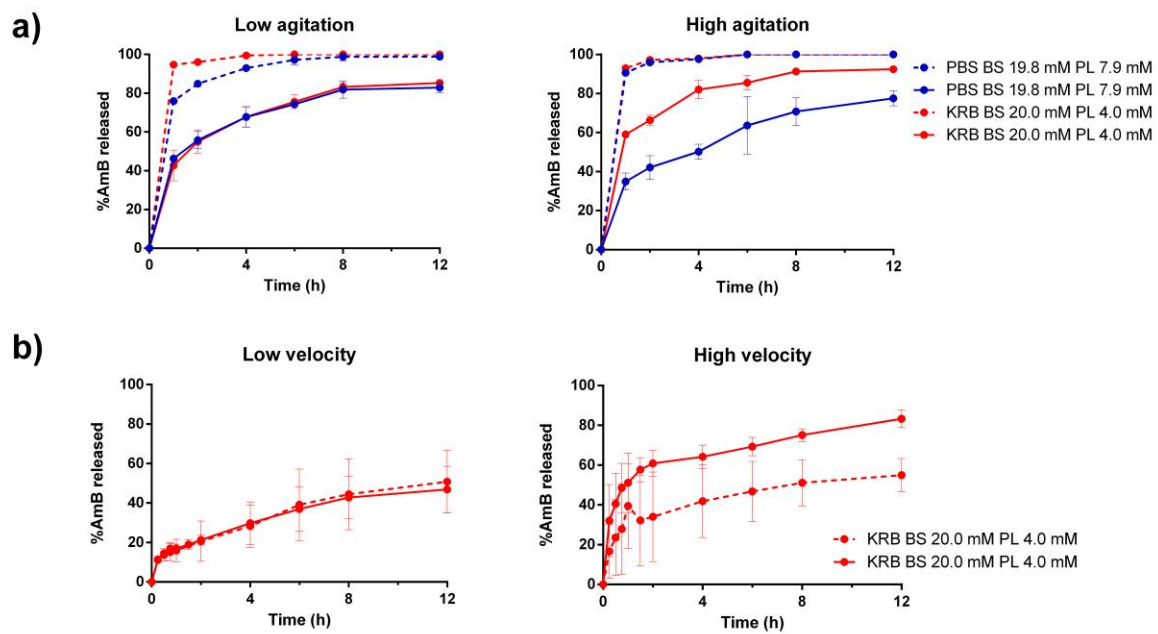


**Figure 3**

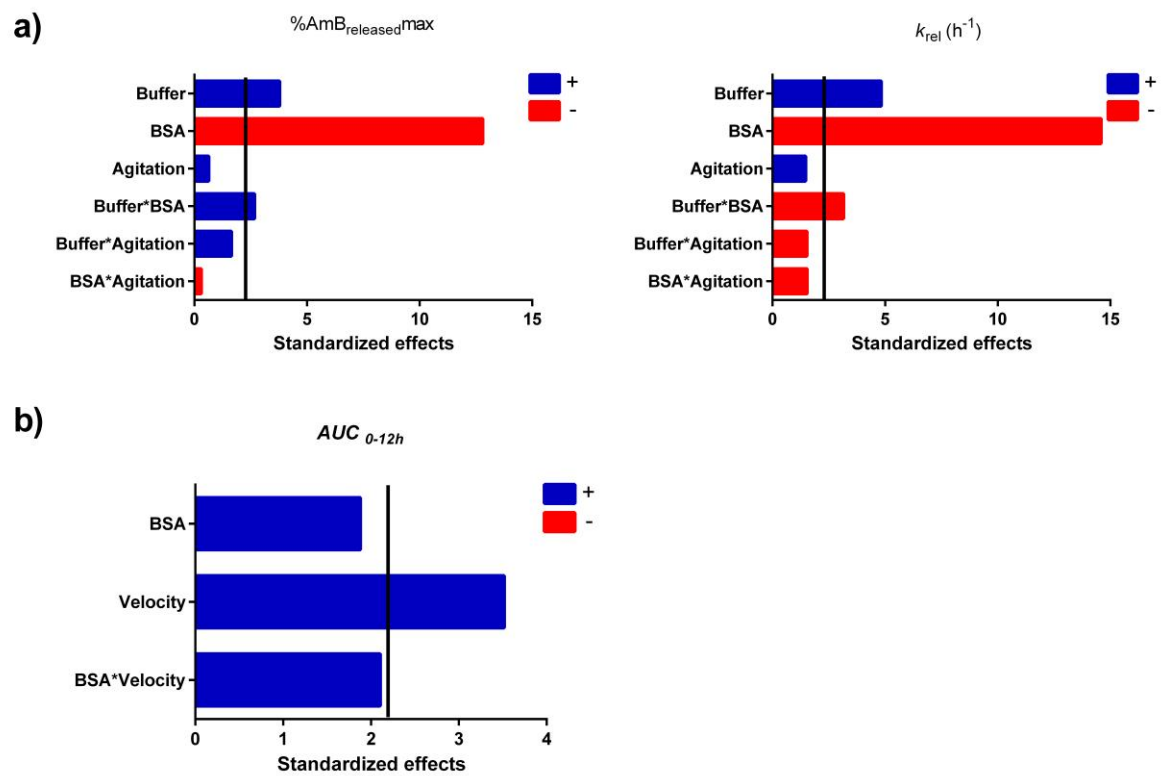


**Figure 4**

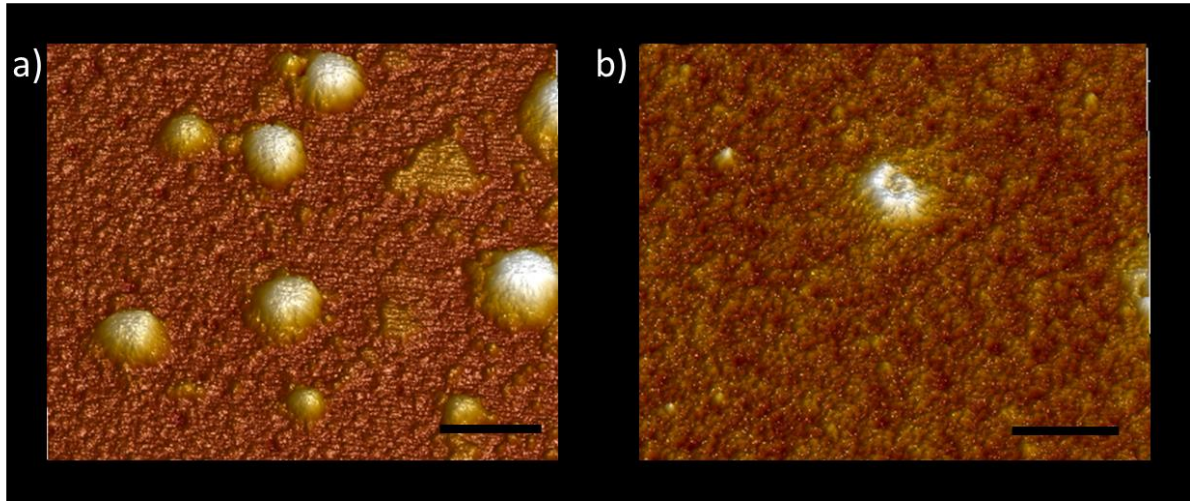


**Figure 5**

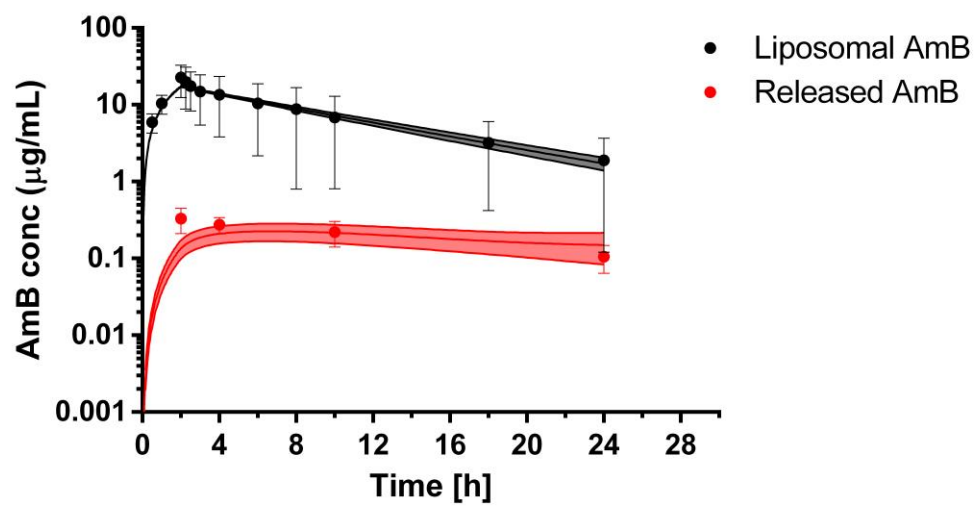
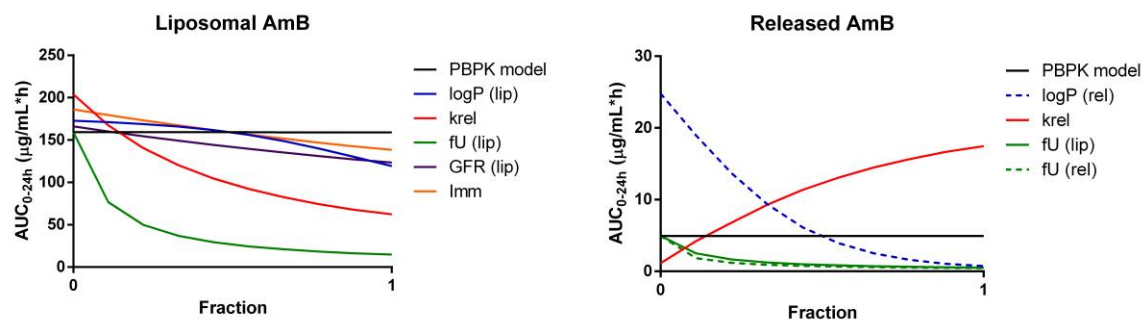


Figure 6



**Figure 7**

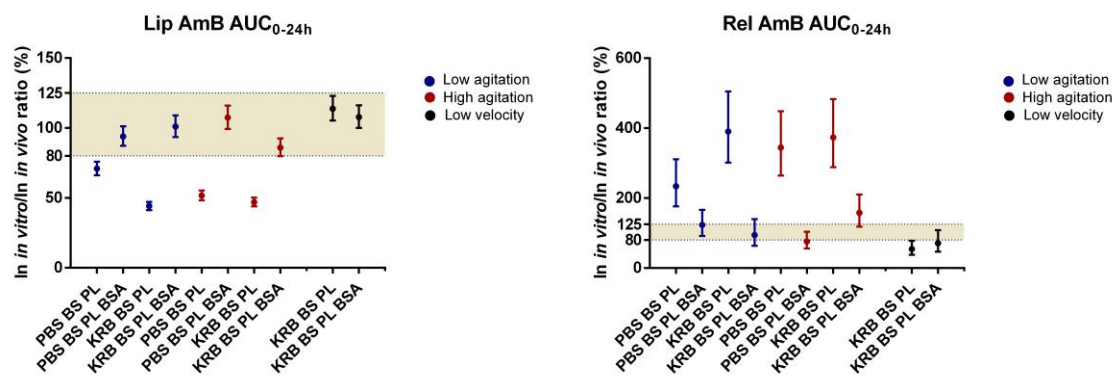
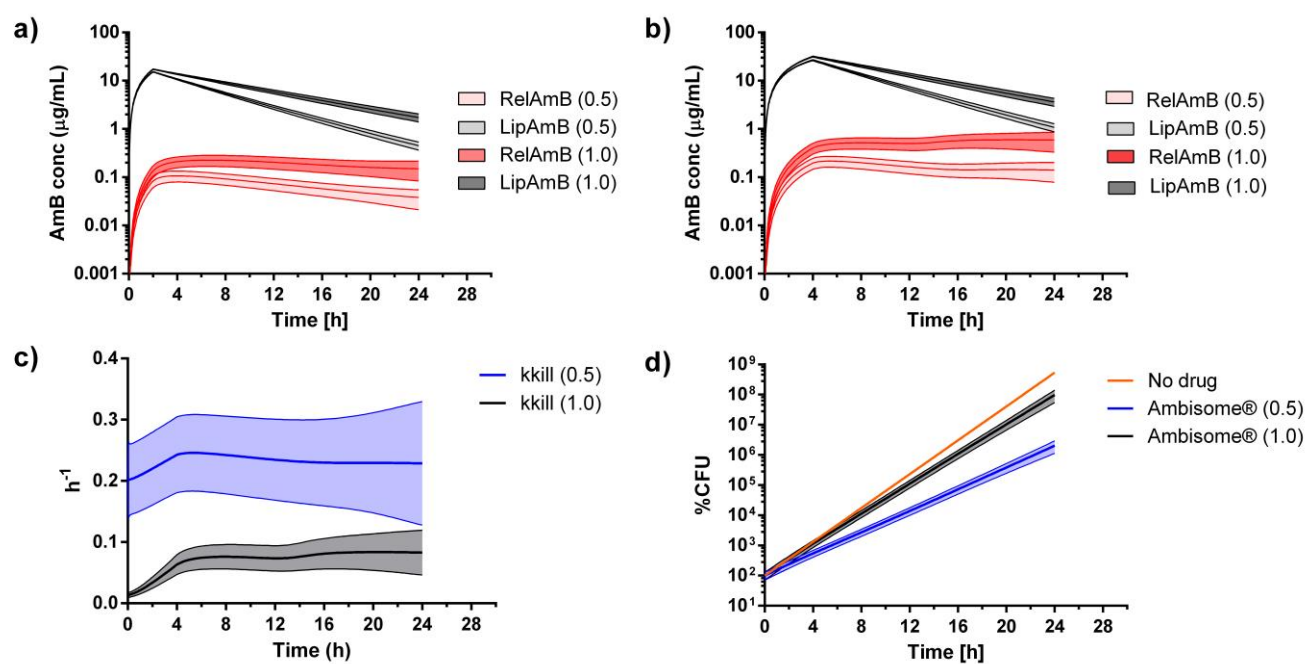


Figure 8





**Figure 9**